TAO/SWIMS サイエンスワークショップ (IoA, Univ of Tokyo, 5/Aug/2013)

SWIMS18サーベイで探る銀河形成の最盛期 (1<z<3 up to 4.5)

児玉　忠恭（国立天文台）

小山佑世（国立天文台）、但木謙一（国立天文台）、林将央（東大宇宙線研）、
嶋川里澄（ハワイ観測所）、田中壱（ハワイ観測所）、他

A galaxy cluster RXJ0152 at z=0.83 (Subaru/Suprime-Cam)

銀河形成最盛期: $1<z<3$ $(6>T_{univ(Gyr)}>2)$

宇宙における銀河やAGNの活動性がピーク！

大局的な星形成率

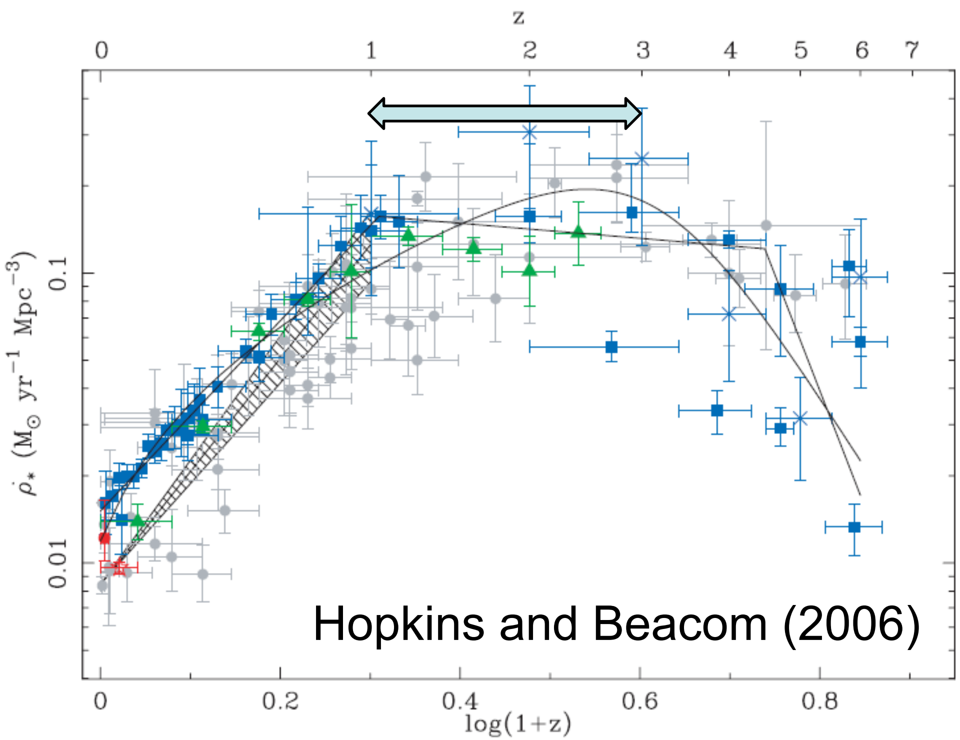

QSOの個数密度

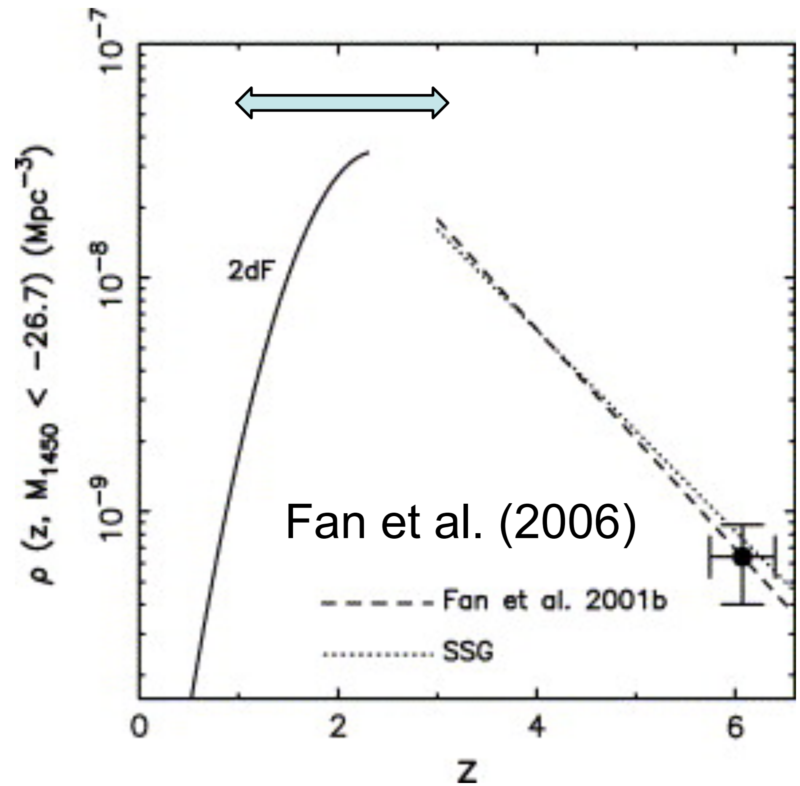

銀河団のRed Sequence や 銀河形態のHubble系列が発現しだす時代。

→ 銀河の屋台骨が作られた、銀河形成＆進化史上、最も重要な時代！

銀河形成最盛期（z～2）研究における近年の目覚ましい進展の数々

- Presence of Dusty Starbursts (SMGs, red HAEs)
- Rapid Decline of Stellar Mass Density
- Emergence of Red Sequence
- Main Sequence of Star Forming Galaxies
- Fundamental Metallicity Relation
- Massive Compact Spheroids (red nuggets)
- Cold Streams (in theory)
- Turbulent, Clumpy, but Rotational Disk
- Gas Outflow (feedback)
- High Ionization State Galaxies (strong [OIII] line)

Stellar mass functions (z)

ULTRA-VISTA (COSMOS)

95,675 galaxies over a 1.62 deg^2 field down to Ks=23.4 (AB)

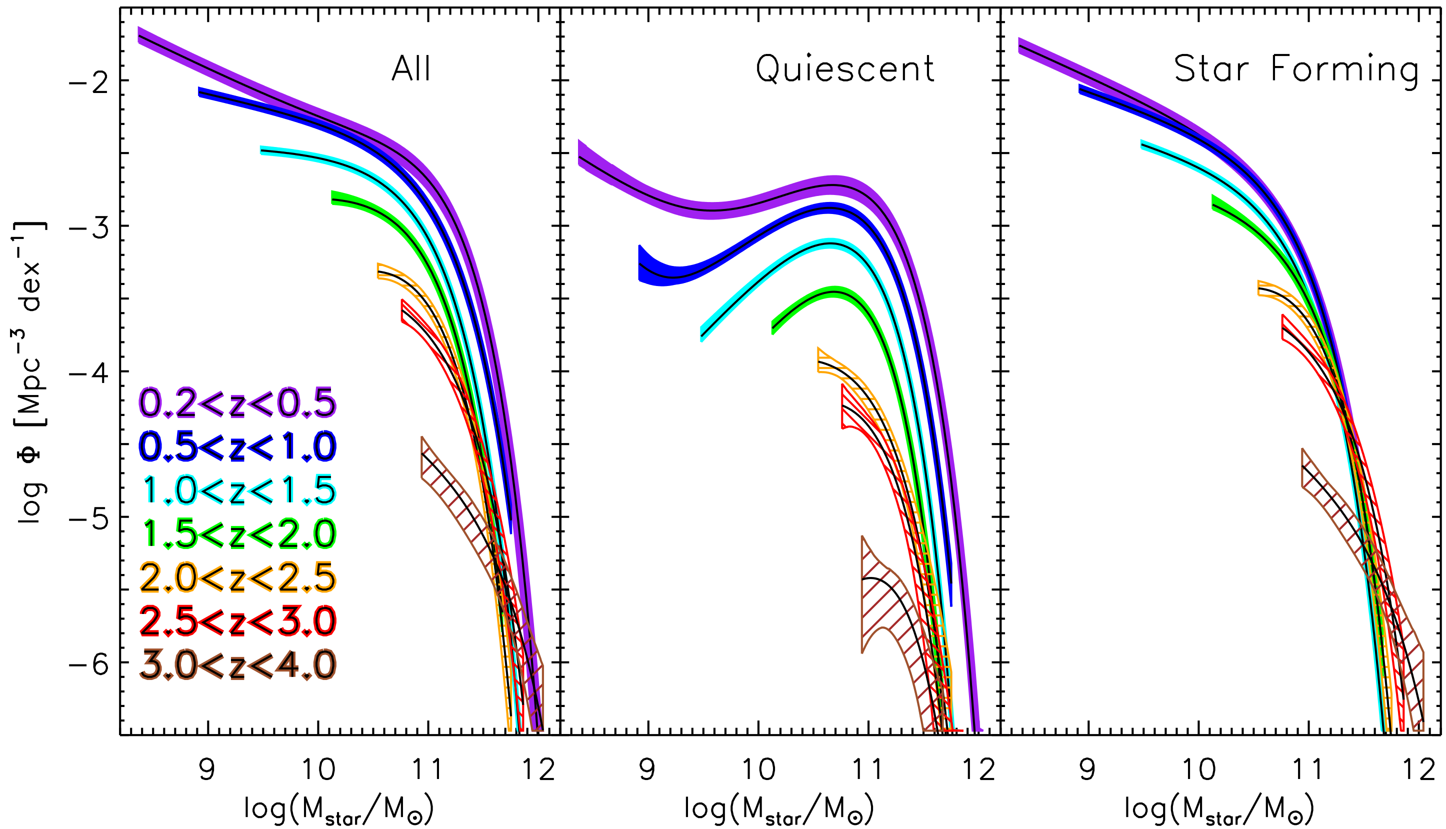

Stellar mass densityは現在に比べ、z=1で50%、z=2で10%、z=3.5で1%にまで下がる。

Muzzin et al. (2013)

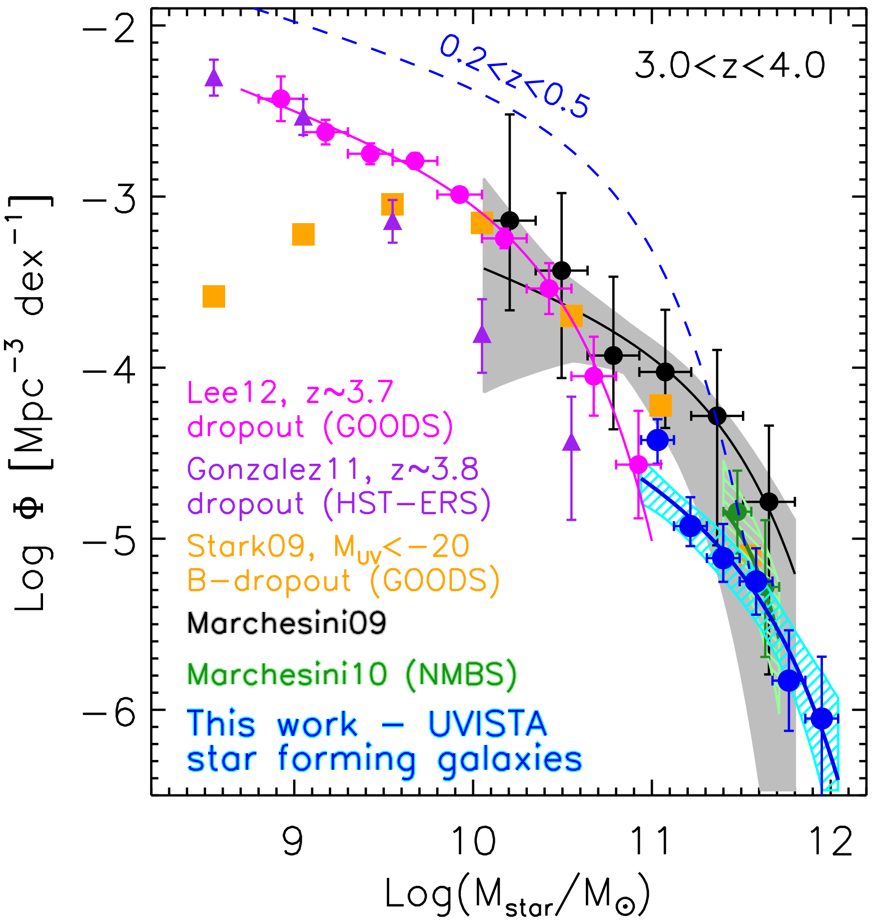

FIG. 12.— Comparison of the K_s-selected SMF of star-forming galaxies at $3.0 < z < 4.0$ from UltraVISTA (blue) and other SMF in the literature. The Marchesini et al. (2009) and Marchesini et al. (2010) SMFs are also K_s-selected samples and agree well with the UltraVISTA SMF. The Stark et al. (2009); González et al. (2011), and Lee et al. (2012) SMFs are UV-selected. These agree reasonably well with UltrsVISTA at $\mathrm{Log}(M_{star}/M_{\odot}) = 11.0$, but it appears the UV-selection may miss the most massive galaxies in this redshift range.

UV-selected samples tend to miss the most massive galaxies !

ULTRA-VISTA (COSMOS)

Muzzin et al. (2013)

“Main Sequence” of Star Forming Galaxies at z~2

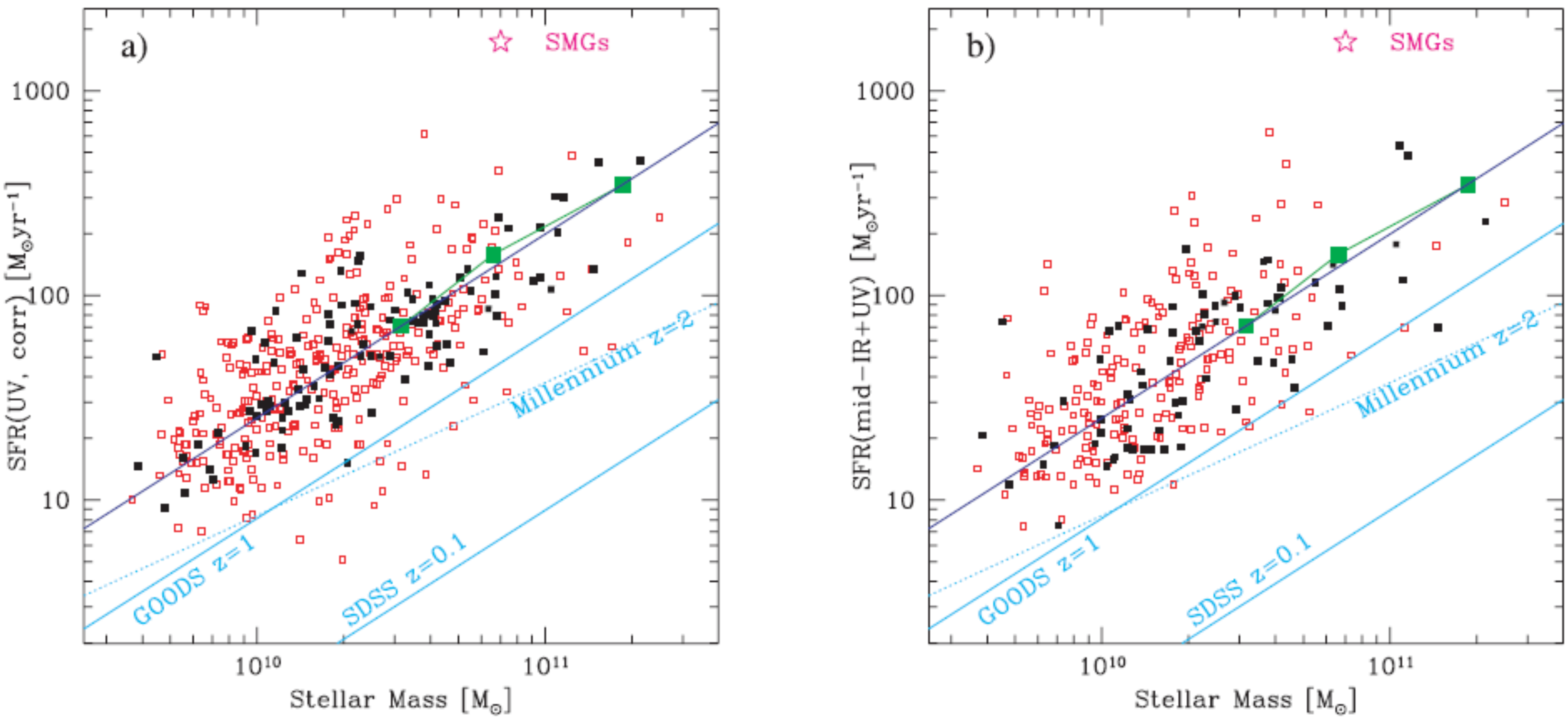

Daddi et al. (2007)

SFR−M*ダイアグラム上での、星形成効率(SFE)と分子ガスの割合

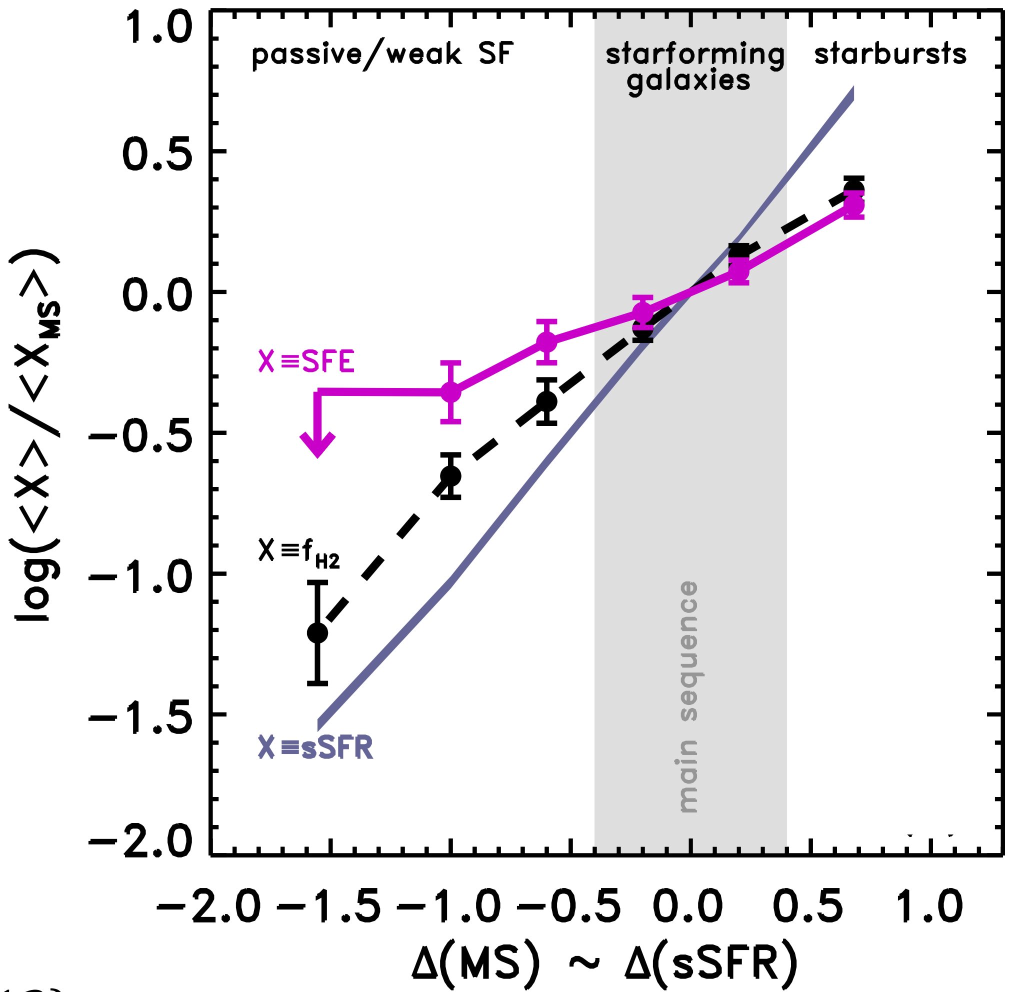

COLDGASS project

SDSS galaxies
IRAM 30-m

Saintonge et al. (2012)

Main Sequenceからの距離の関数として、分子ガス割合も、星形成効率も、共に高くなる。

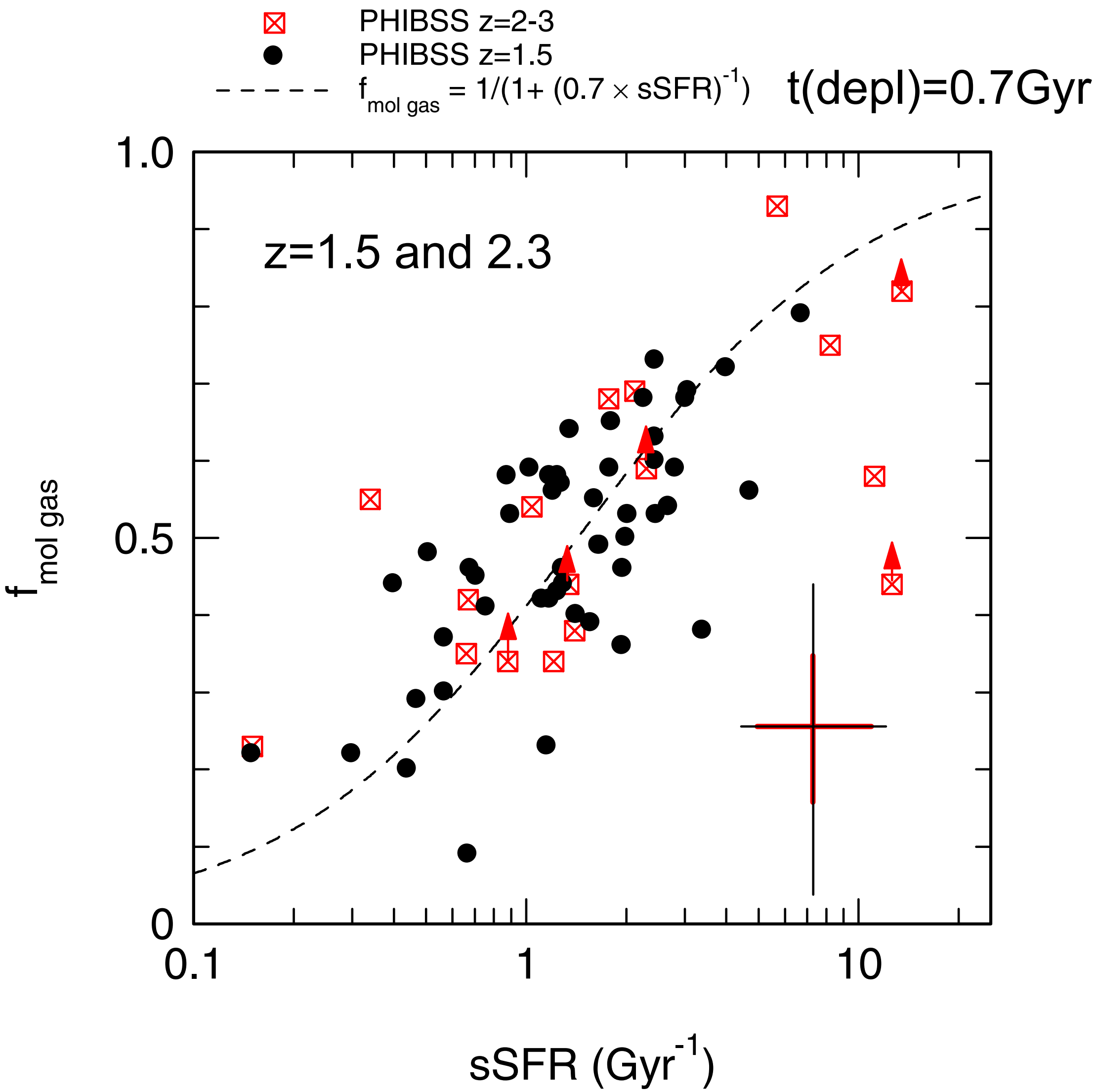

Gas fraction vs. sSFR

Clear correlation!
Depletion time scale~0.7Gyr
Need continuous gas supply!

Main sequenceや
Fundamental metallicity relation
の分散にはgas fractionの違いが
大きく寄与（主要因？）

一方で分散もあり、SFEも寄与？

$$f_{\mathrm{mol\ gas}} = \frac{M_{\mathrm{mol\ gas}}}{M_{\mathrm{mol\ gas}} + M_*} = \frac{1}{(1 + [\mathrm{sSFR} \times t_{\mathrm{depl}}]^{-1})}$$

Tacconi et al. (2013)

Massive, compact, spheroidal galaxies at z>2

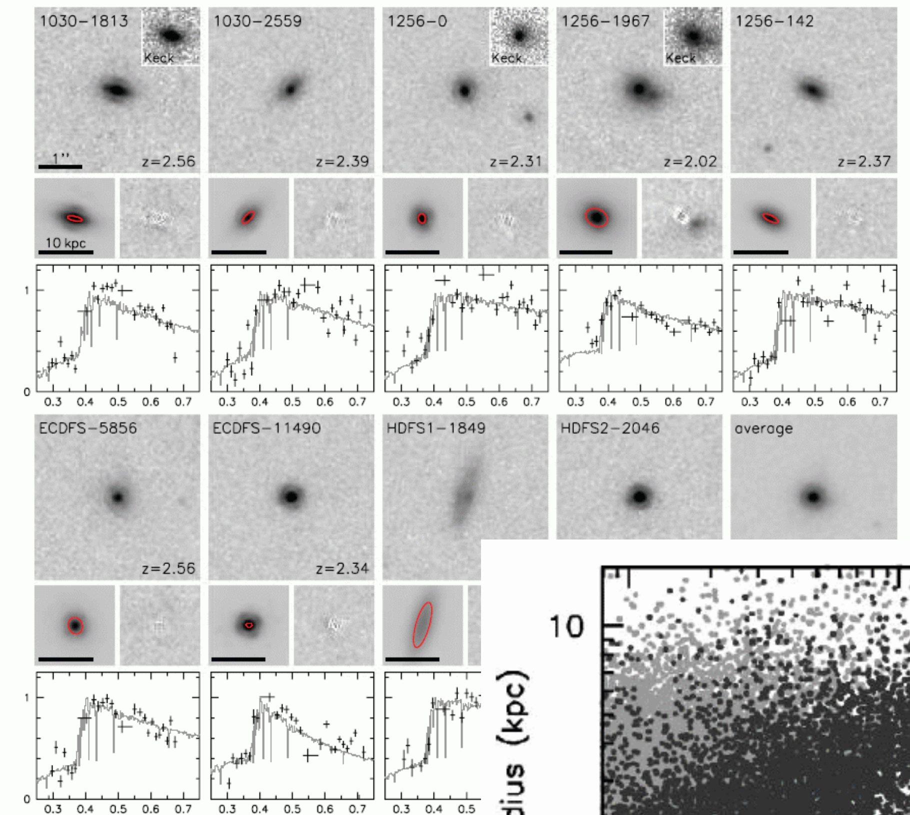

"red nuggets"

Median stellar mass: $1.7 \times 10^{11} M_\odot$
Median effective radius: 0.9 kpc

Sizes are x5 smaller, and densities are 2 orders higher than nearby ellipticals!

HST/NIC2
Keck/LGS-AO

van Dokkum et al. (2008)

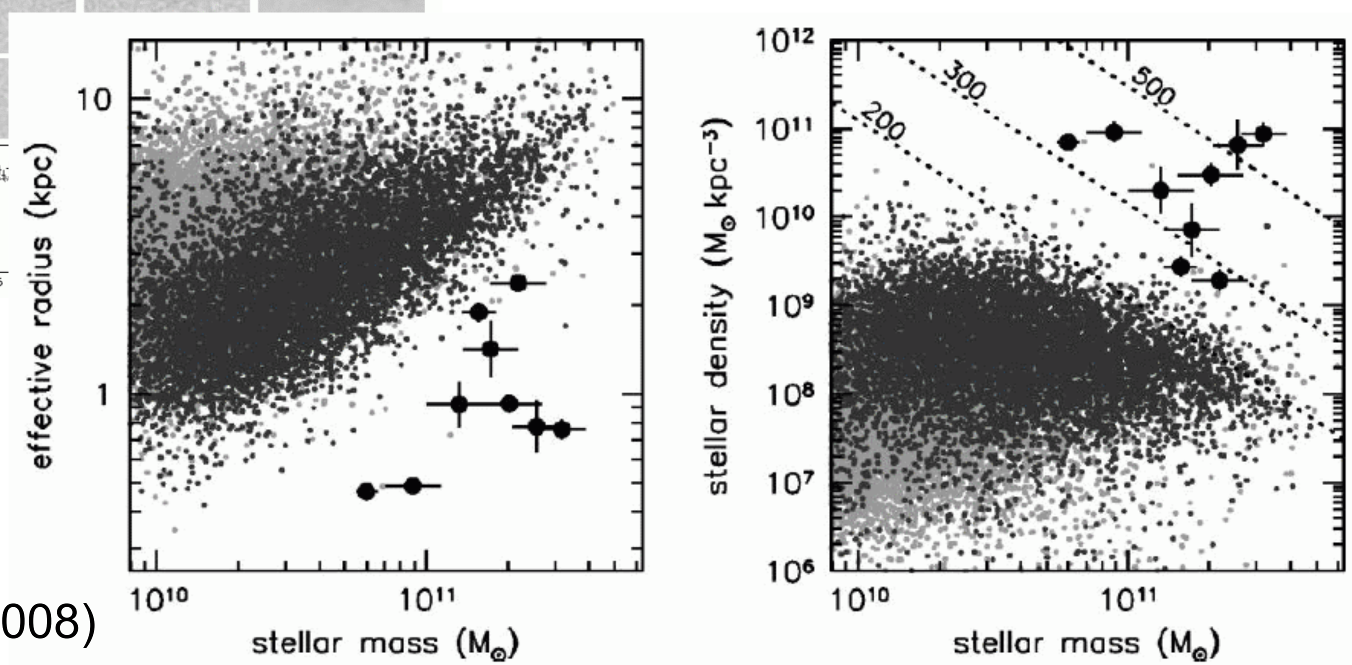

大質量銀河($M>10^{11}M_\odot$)のサイズと質量進化

Size growth

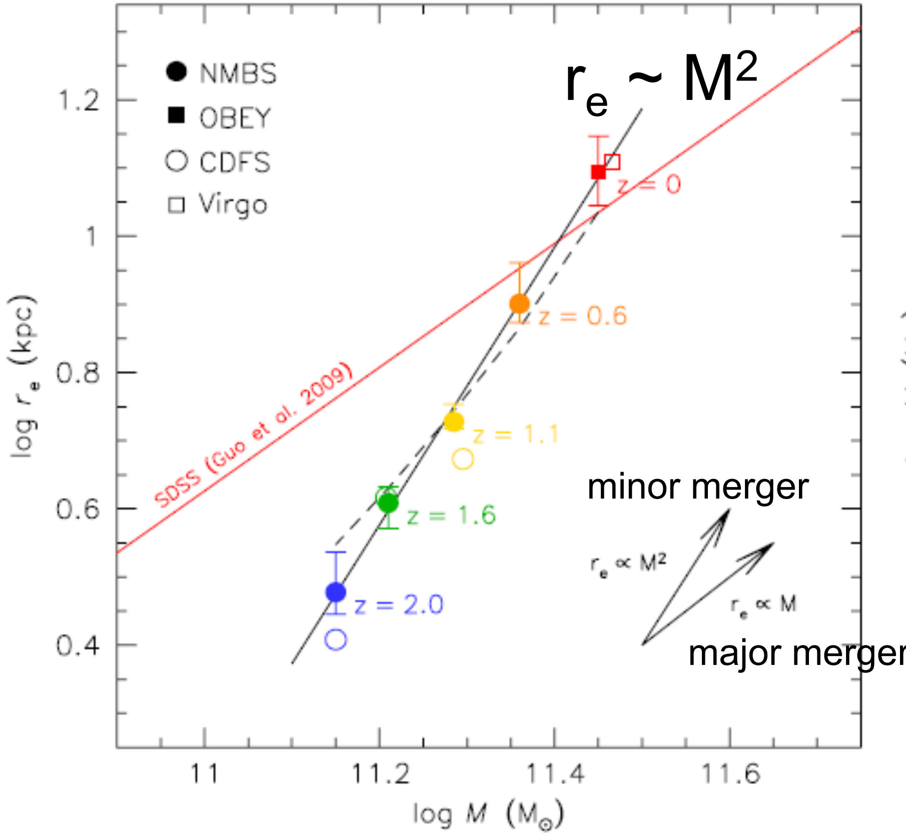

Figure 8. Evolution in the radius–mass plane. Our data are consistent with measurements for individual galaxies of the same masses and redshifts in the FIREWORKS CDF-South survey of Wuyts et al. (2008) and Franx et al. (2008) (open circles). Our $z = 0$ point from the OBEY survey (Tal et al. 2009) is consistent with data from Virgo ellipticals by Kormendy et al. (2009) and a recent determination of the mass–size relation in the SDSS (Guo et al. 2009). The evolution in effective radius is stronger than in mass: the solid line is a fit of the form $r_e \propto M^{2.04}$. The dashed line is the expected evolution of the effective radius for inside-out growth, calculated using Equation (7) and the measured value of the Sersic index n at each redshift.

Mass growth

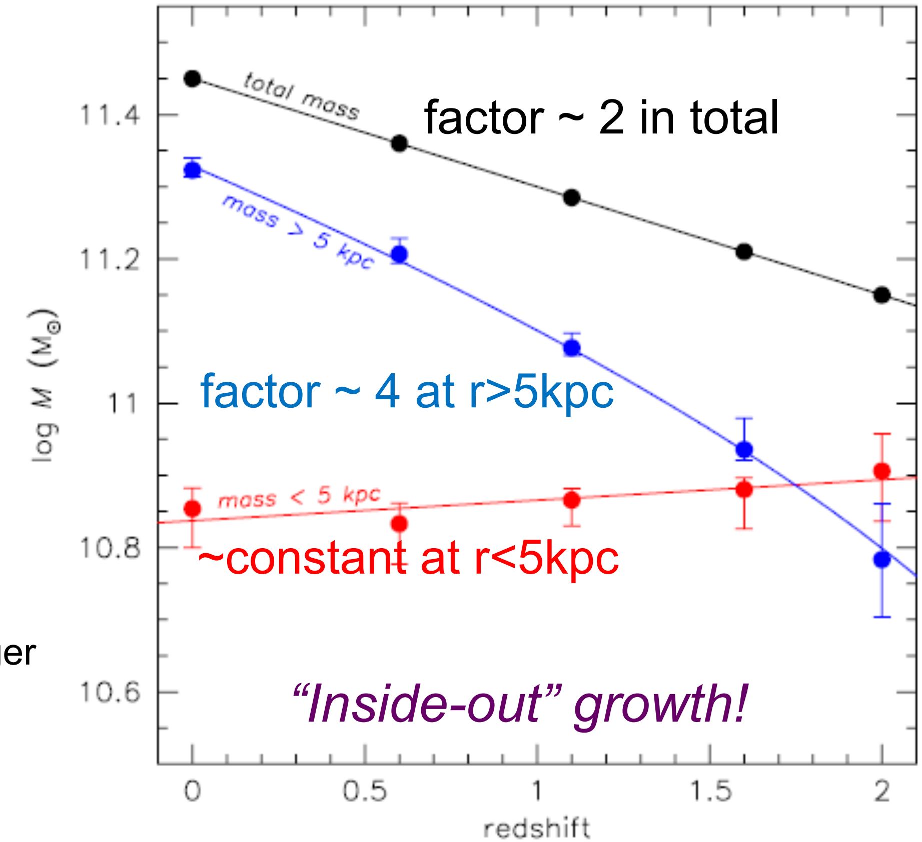

Figure 9. Comparison of the mass contained within a fixed radius of 5 kpc (red curve) to the mass at larger radii (blue curve), as a function of redshift. Error bars are 95% confidence limits derived from bootstrapping. The total mass is shown in black. Galaxies with number density $n = 2 \times 10^{-4}$ Mpc^{-3} have a nearly constant mass in the central regions. The factor of ≈2 increase in total mass since $z = 2$ is driven by the addition of stars at radii >5 kpc.

NEWFIRM medium-band survey
van Dokkum et al. (2010)

“MAHALO-Subaru”

MApping HAlpha and Lines of Oxygen with Subaru

Unique sample of NB selected SF galaxies across environments and cosmic times

	environ-ment	target	z	line	λ (μm)	camera	NB-filter	conti-nuum	status as of Oct ’12
z<1 cluster	Low-z cluster	CL0024+1652	0.40	Hα	0.916	S-Cam	NB912	z'	Kodama+’04
		CL0939+4713	0.41	Hα	0.923	S-Cam	NB921	z'	Koyama+’11
		RXJ1716.4+6708	0.81	Hα	1.190	MOIRCS	NB1190	J	Koyama+’10
				[OII]	0.676	S-Cam	NA671	R	observed
z~1.5 cluster	High-z cluster	XCSJ2215–1738	1.46	[OII]	0.916	S-Cam	NB912,921	z'	Hayashi+’10,’11
		4C65.22	1.52	Hα	1.651	MOIRCS	NB1657	H	observed
		CL0332–2742	1.61	[OII]	0.973	S-Cam	NB973	y	Hayashi+’13
		CIGJ0218.3–0510	1.62	[OII]	0.977	S-Cam	NB973	y	Tadaki+’12
z~2 cluster	Proto-cluster	PKS1138–262	2.16	Hα	2.071	MOIRCS	NB2071	K_s	Koyama+’12
		4C23.56	2.48	Hα	2.286	MOIRCS	NB2288	K_s	Tanaka+’11
		USS1558–003	2.53	Hα	2.315	MOIRCS	NB2315	K_s	Hayashi+’12
z~2 field	General field	GOODS-N	2.19	Hα	2.094	MOIRCS	NB2095	K_s	Tadaki+’11
		(70 arcmin^2)		Hβ	1.551	MOIRCS	NB1550	H	not yet
				[OII]	1.189	MOIRCS	NB1190	J	observed
		SXDF-CANDELS	2.19	Hα	2.094	MOIRCS	NB2095	K	Tadaki+’13
		(92 arcmin^2)		Hβ	1.551	MOIRCS	NB1550	H	not yet
				[OII]	1.189	MOIRCS	NB1190	J	not yet
			2.53	Hα	2.315	MOIRCS	NB2315	K_s	Tadaki+’13

18 nights for imaging, >15 nights for spectroscopy

Unique Sets of Narrow-Band Filters on Wide-Field Cameras
Suprime-Cam (optical) and MOIRCS (NIR)

The existing Suprime-Cam NB-filters capture emission lines from known good targets.
The MOIRCS NB-filters were specifically designed for good targets at frontier redshifts.

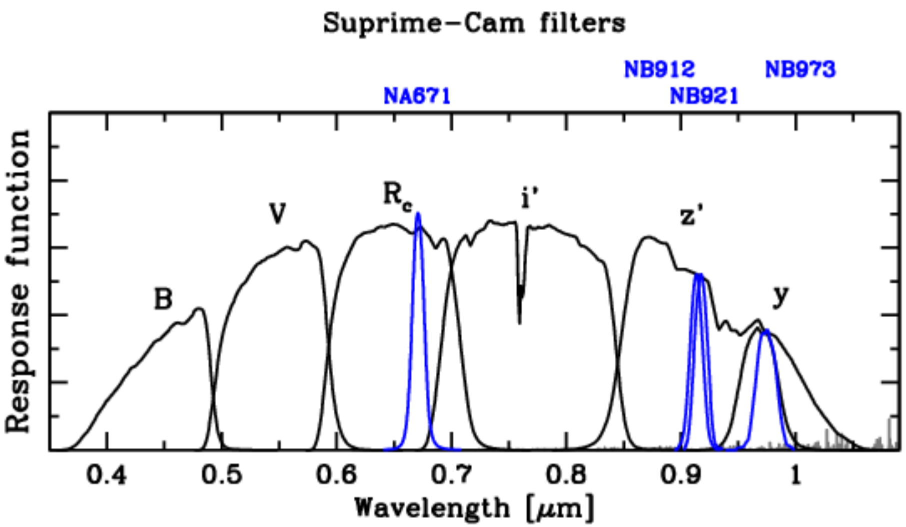

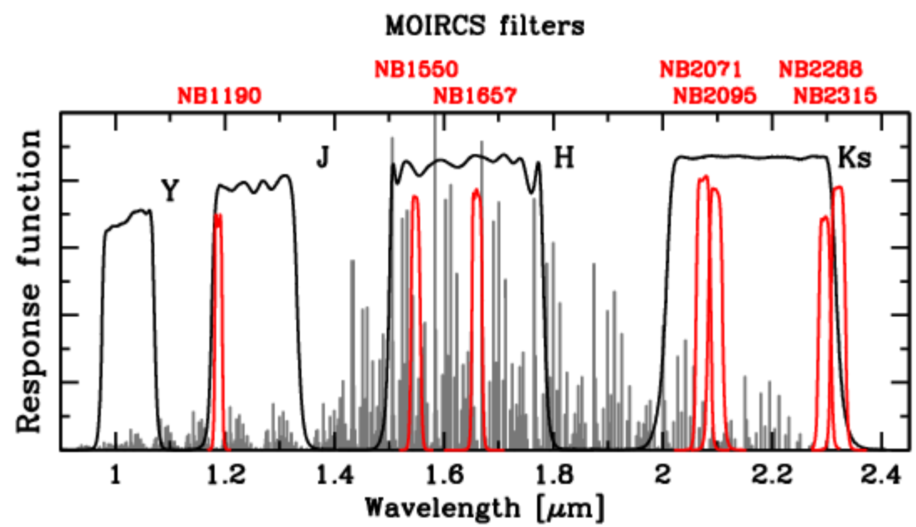

4 narrow-band filters

7 narrow-band filters

Camera	Filter	λ_c	FWHM
MOIRCS	NB1190	1.189μm	0.014μm
	NB1550	1.550μm	0.018μm
	NB1657	1.657μm	0.019μm
	NB2071	2.069μm	0.027μm
	NB2095	2.095μm	0.025μm
	NB2288	2.296μm	0.023μm
	NB2315	2.313μm	0.027μm
Suprime-Cam	NA671	0.6714μm	0.0130μm
	NB912	0.9139μm	0.0134μm
	NB921	0.9173μm	0.0132μm
	NB973	0.9755μm	0.020μm

FWHMs correspond to ±1500-2000km/s

Clean selection of SFGs (line emitters) by NB imaging

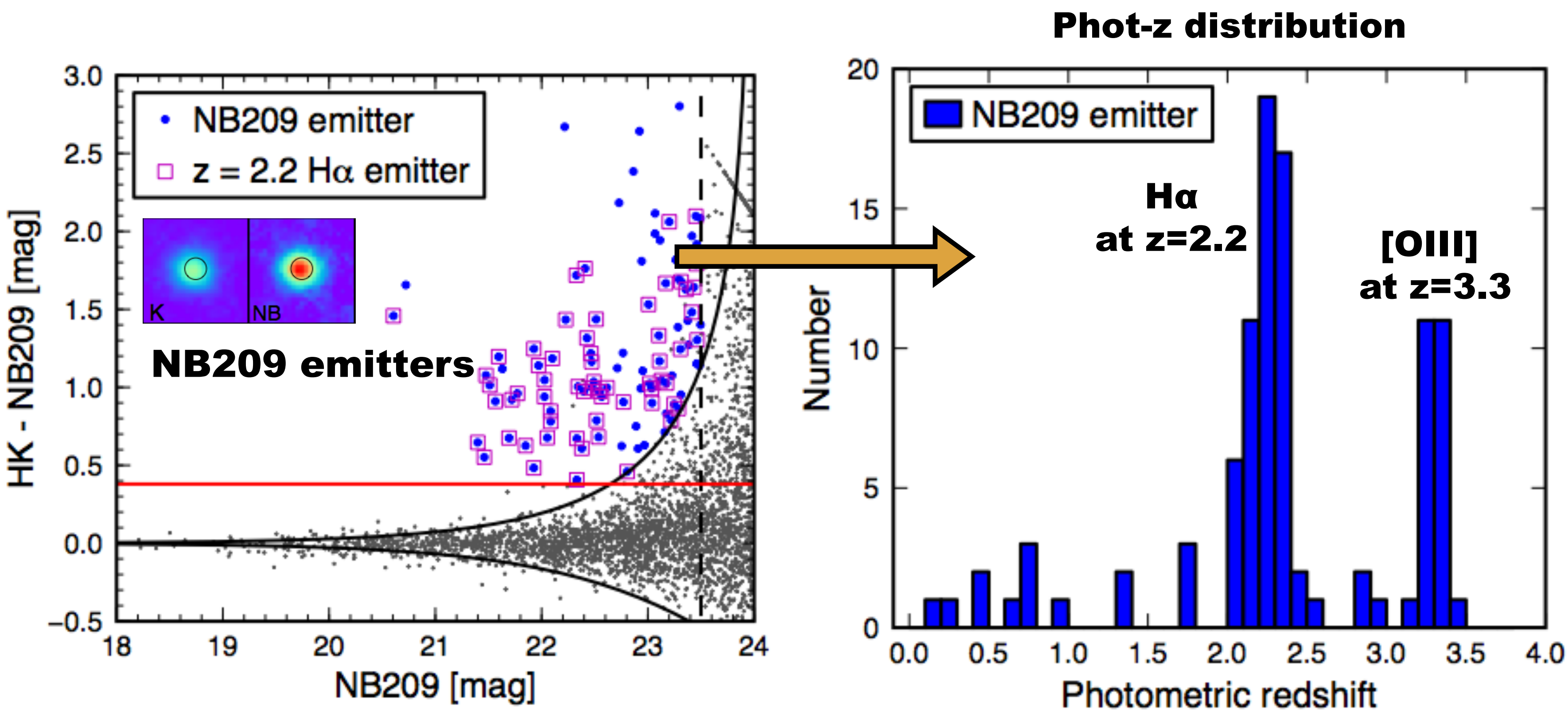

Tadaki et al. (2013a)

An ancient city of galaxies under rapid construction

USS1558-003 (z=2.53)

Ha imaging
with MOIRCS/NB2315
3.4 hrs, 0.3-0.4" seeing

68 Ha emitters (HAEs) are detected.

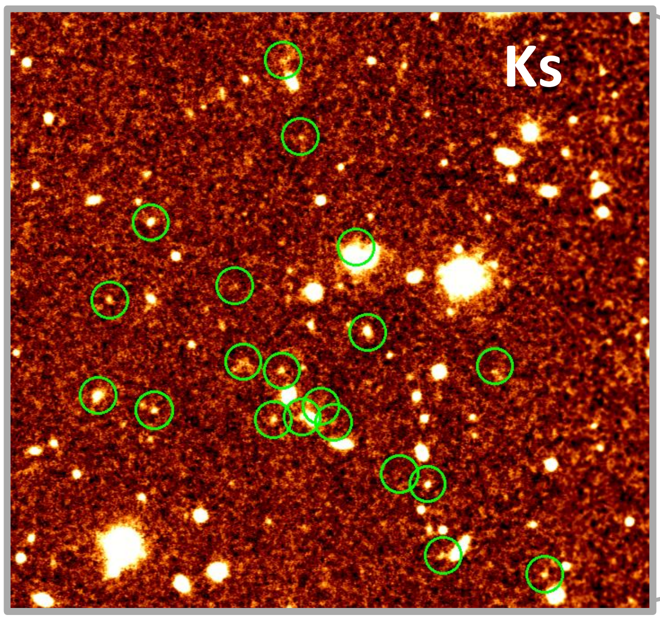

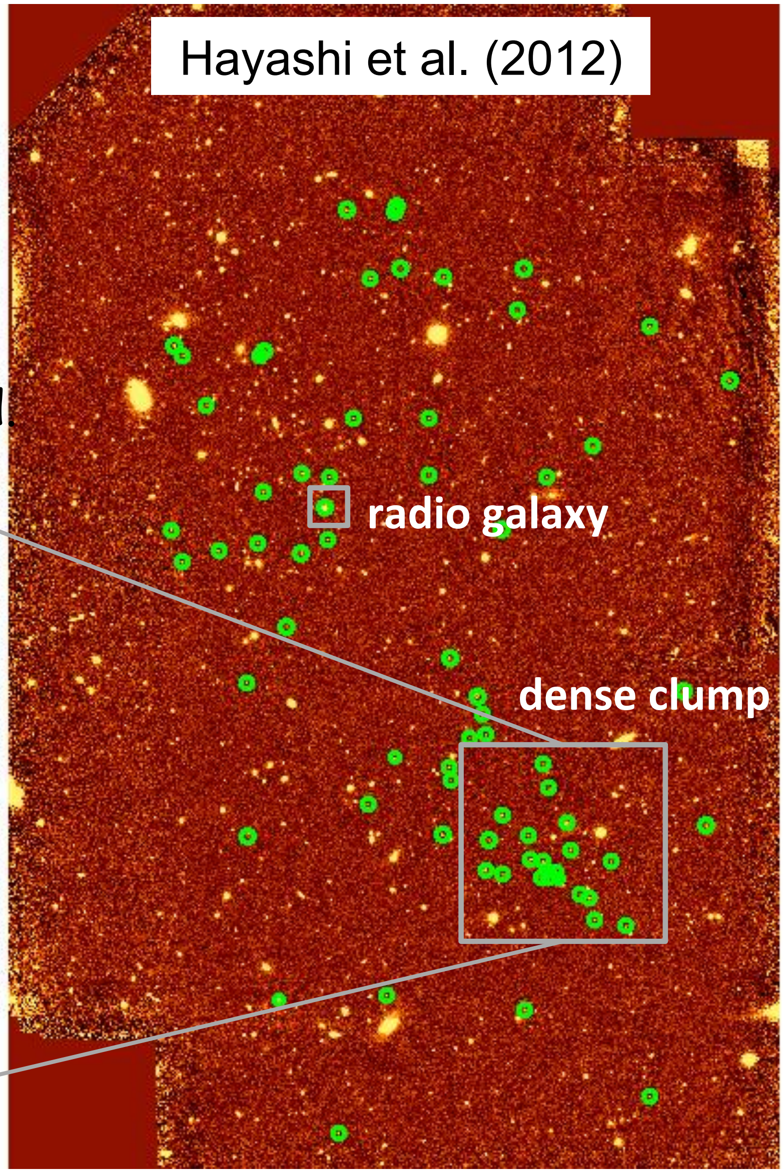

1.5Mpc away from the RG

~20x denser than the general field.
Mean separation between galaxies is ~150kpc.

A star-bursting proto-cluster!

Clusters Grow Inside-Out !

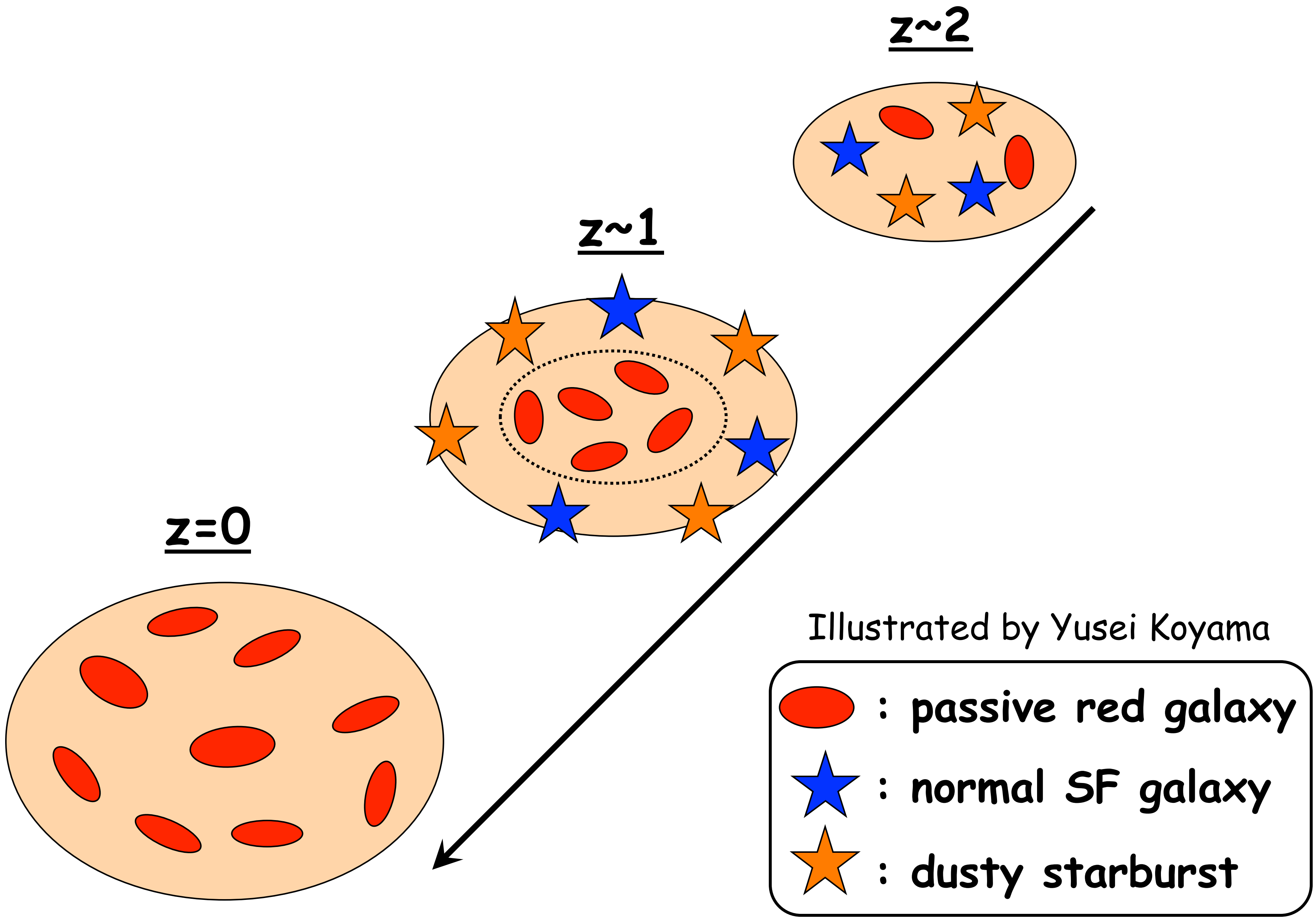

星形成銀河のMain Sequenceの環境依存性 @z=2

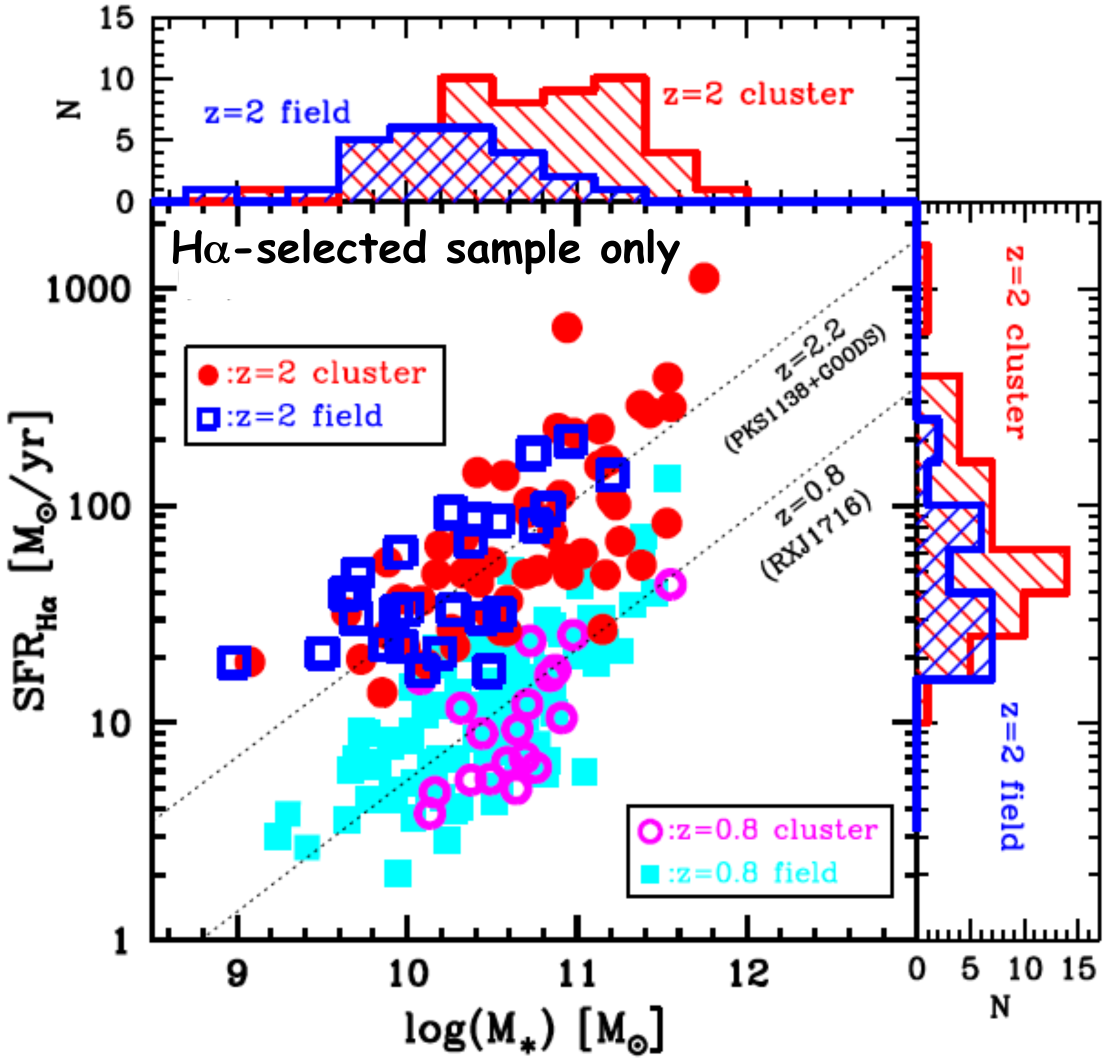

M*-dependent dust correction for Hα is applied.
(Garn & Best 2010)

原始銀河団(PKS1138 at z~2)の星形成銀河は、フィールドと同じ"Main Sequence"に載る。

しかし、

MS上での銀河の分布は異なり、原始銀河団の方がより質量のが大きい（星形成率が高い）側に偏った分布をしている。

→ 高密度領域での加速的な銀河形成を示唆

Koyama et al. (2013a)

SF galaxies at the peak epoch @SXDF-UDS-CANDELS

z=2.2 Hα emitters
(NB2095)

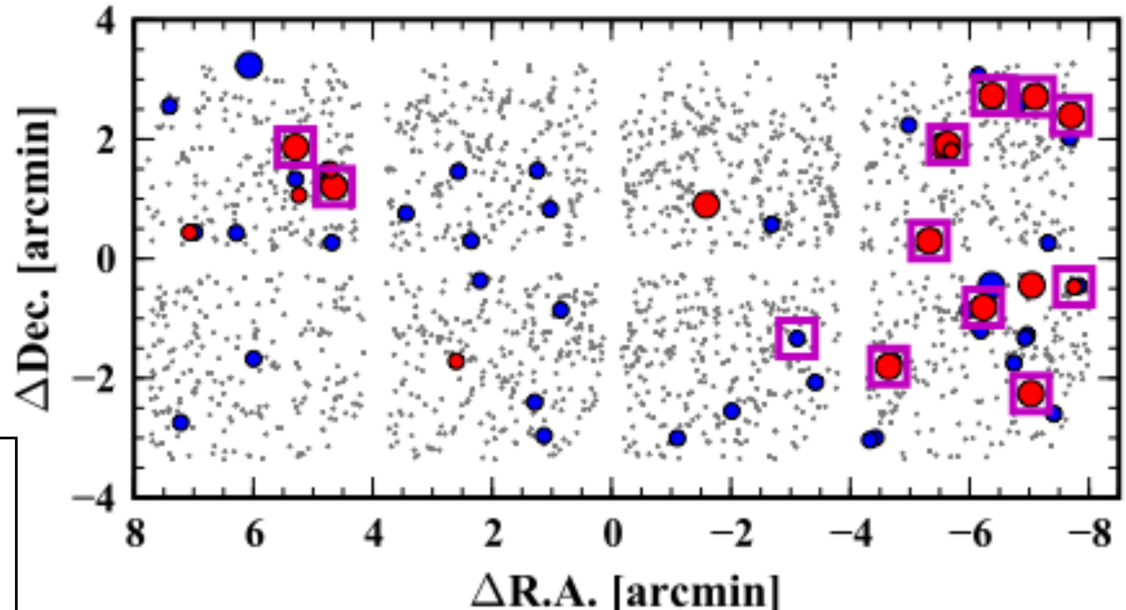

● : blue HAE (J-K<1)
● : red HAE (J-K>1)
□ : MIPS sources
(dusty star-bursting galaxies)

z=2.5 Hα emitters
(NB2315)

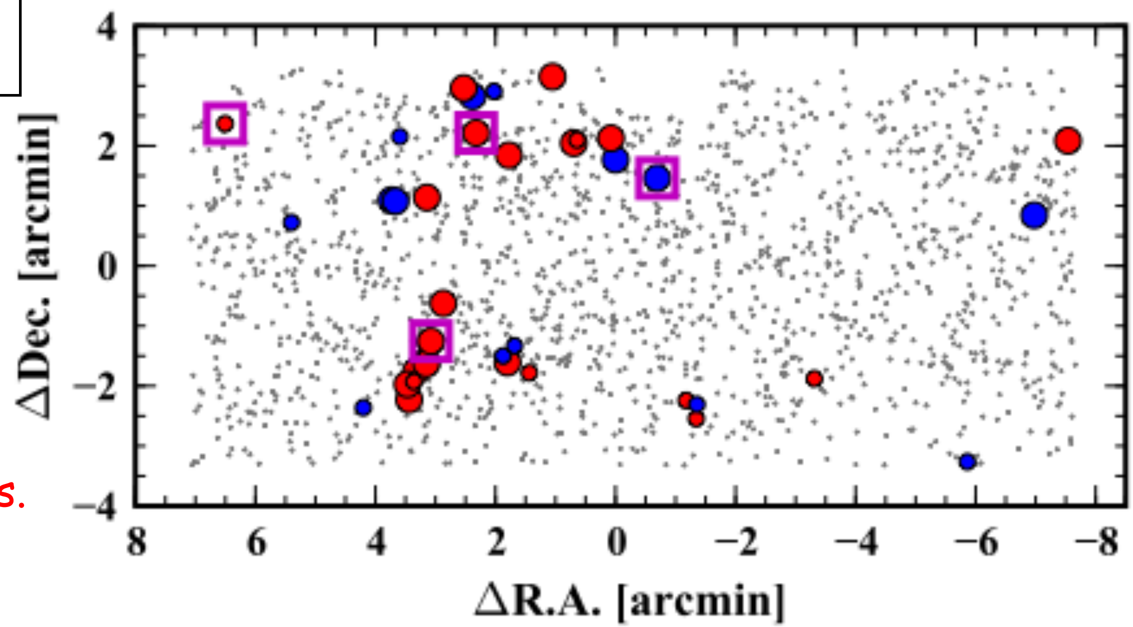

HAEs are strongly structured,
in particular the red HAEs/MIPS
sources favor high density regions.

Tadaki et al. (2013b)

Clumpy Structure is Common

~40% of HAEs at z~2 show clumpy (or merger) structures

HST images (V_{606},I_{814},H_{160}) from the CANDELS survey

less massive clumpy galaxies ($M_{star}<10^{10}M_{\odot}$) | **massive clumpy galaxies** ($M_{star}=10^{10-11}M_{\odot}$)

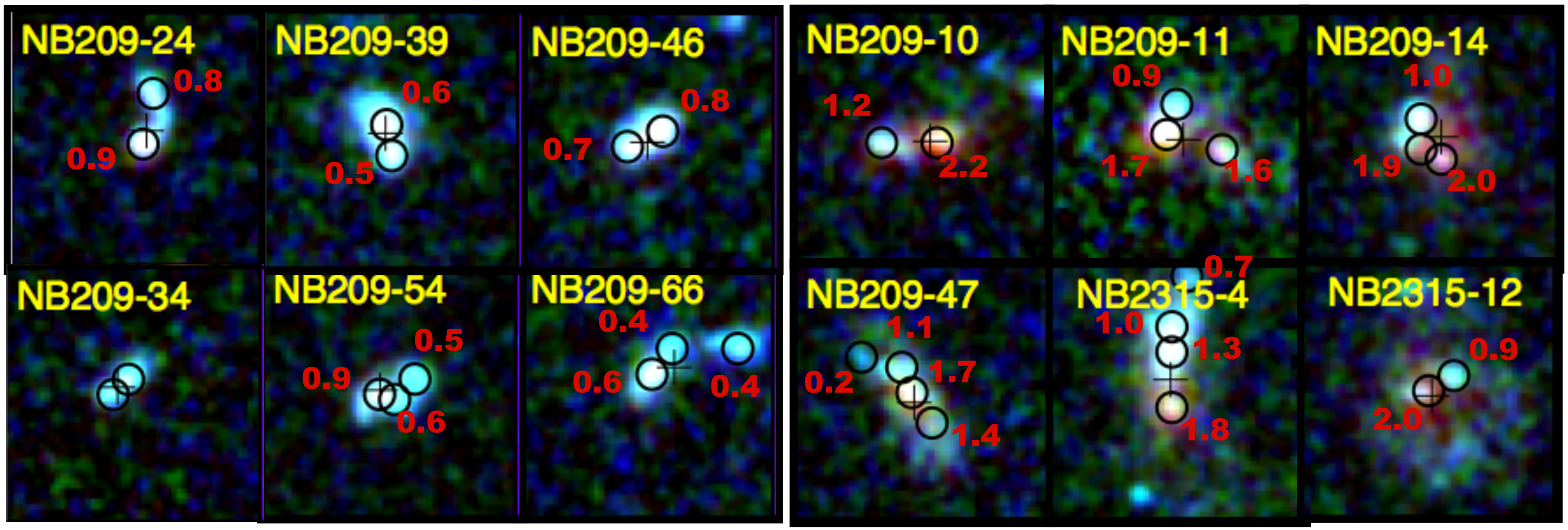

colours (I_{814}-H_{160}) of individual clumps are shown with red numbers

Tadaki et al. (2013b)

Massive clumpy galaxies tend to have a red clump near the stellar-mass center, which may be hosting a central dusty starburst and forming a bulge eventually !

Environmental dependence of the clumpiness and their colours is expected!

Size-Mass Relation of NB(Hα)-selected SF Galaxies at z~2

in SXDF-UDS-CANDELS field

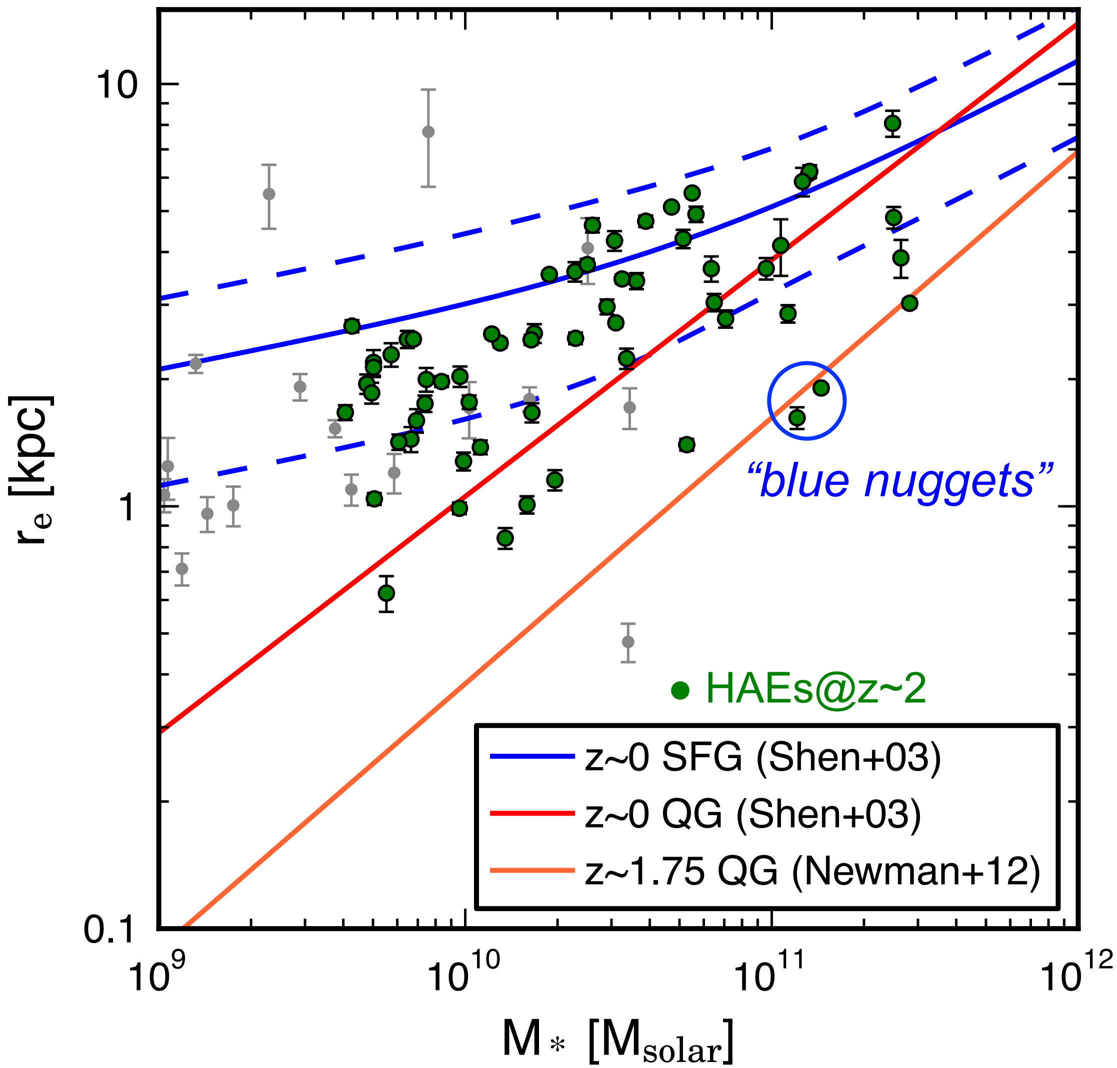

* Not much evolution is seen in global mass-size relation since z~2 to z=0.

* Two blue nuggets are found which are likely to be direct precursors of red nuggets seen at z~1-2

Tadaki et al. (2013)

Two Channels for Formation of Massive Quiescent Galaxies

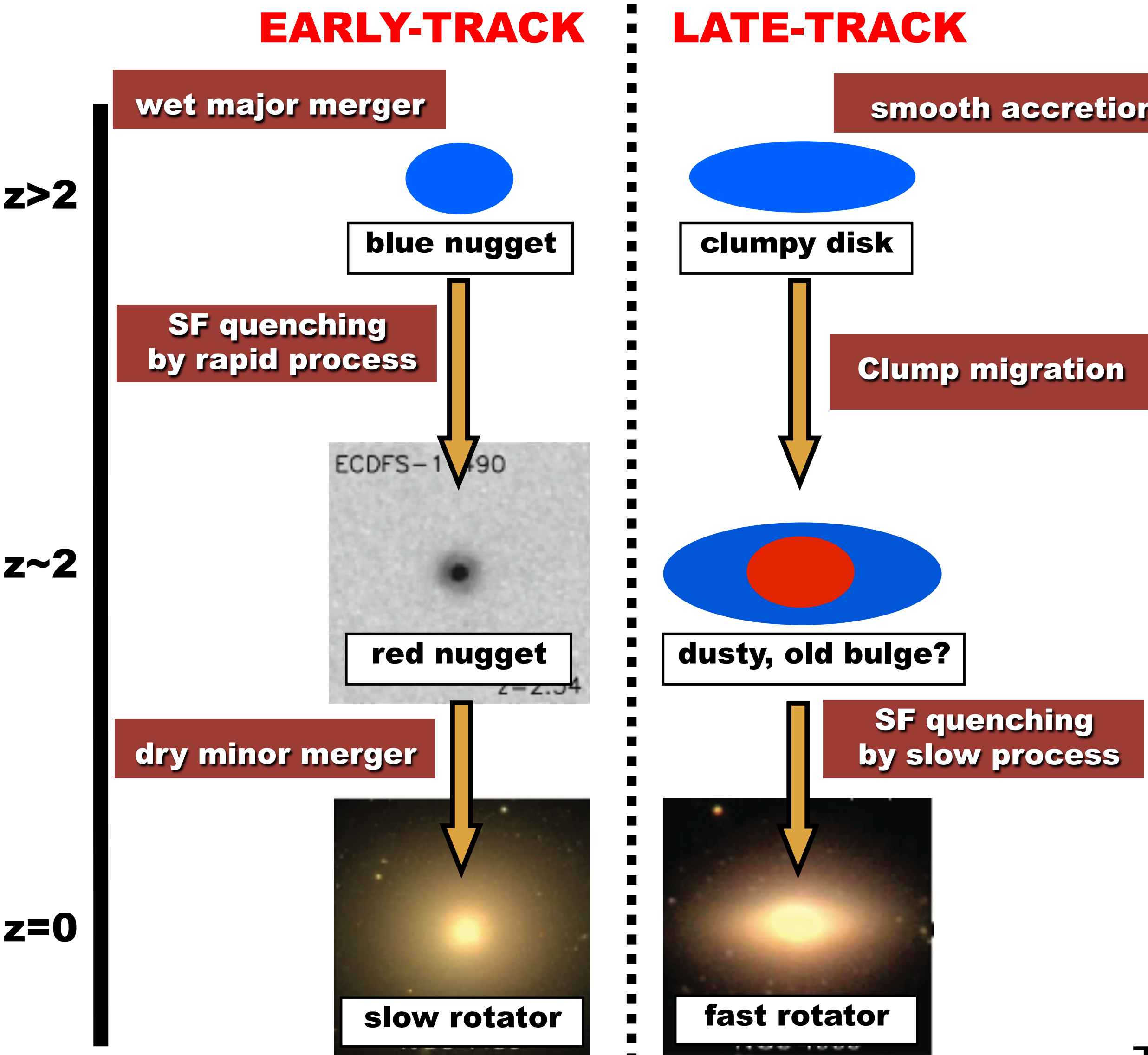

Barro+13

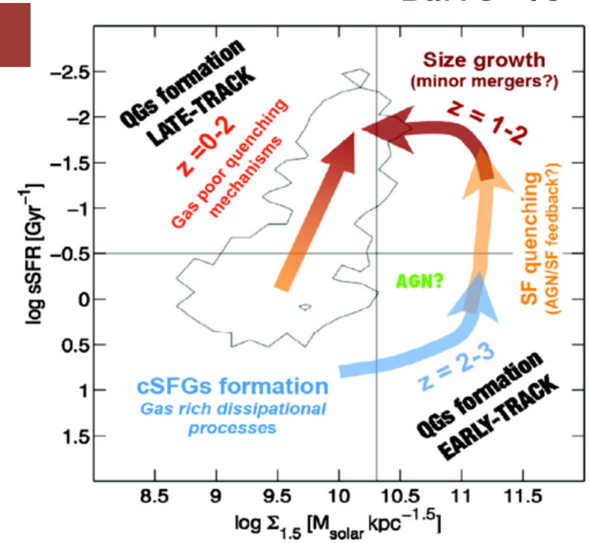

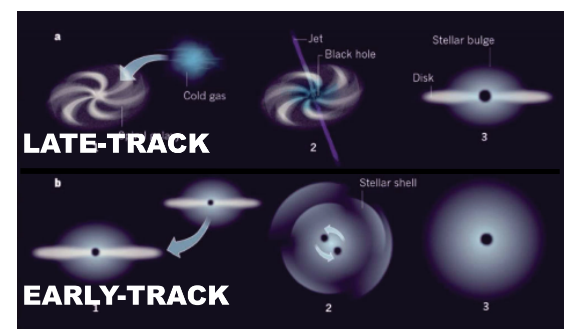

Cappellari+13

Tadaki et al. (2013b)

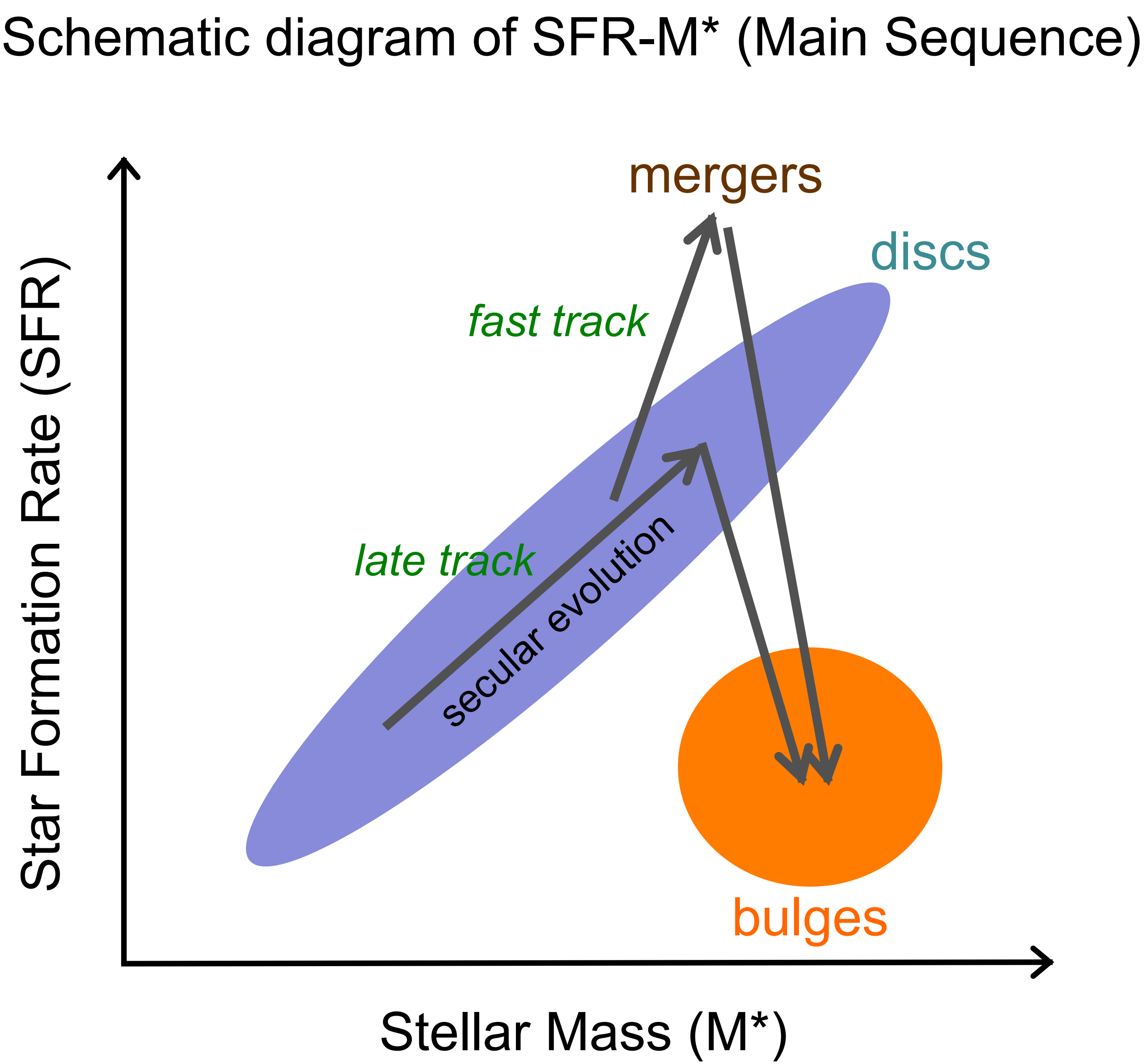

Schematic diagram of SFR-M* (Main Sequence)
mergers
discs
fast track
late track
secular evolution
bulges
Star Formation Rate (SFR)
Stellar Mass (M*)

PKS1138 member (z=2.16)

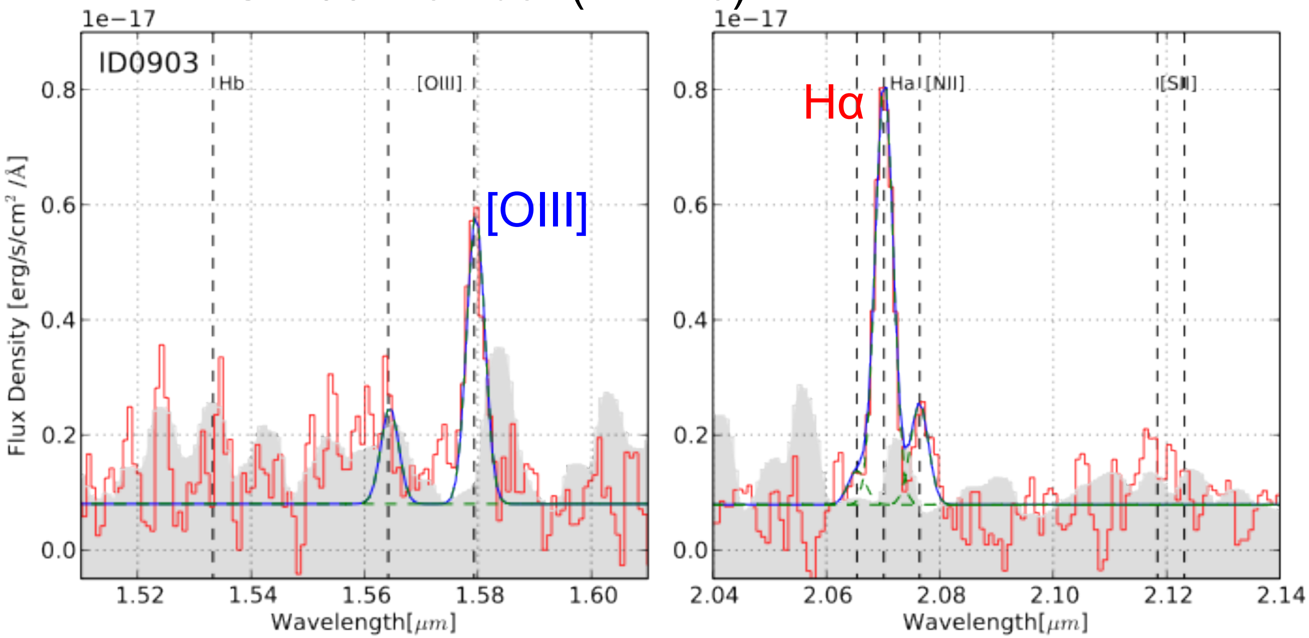

最近、遠方銀河(z>2)で[OIII]が強くなっているケースが報告されている。

物理状態は？
（重元素量が低い？
AGNの寄与？他？）

USS1558 member (z=2.53)

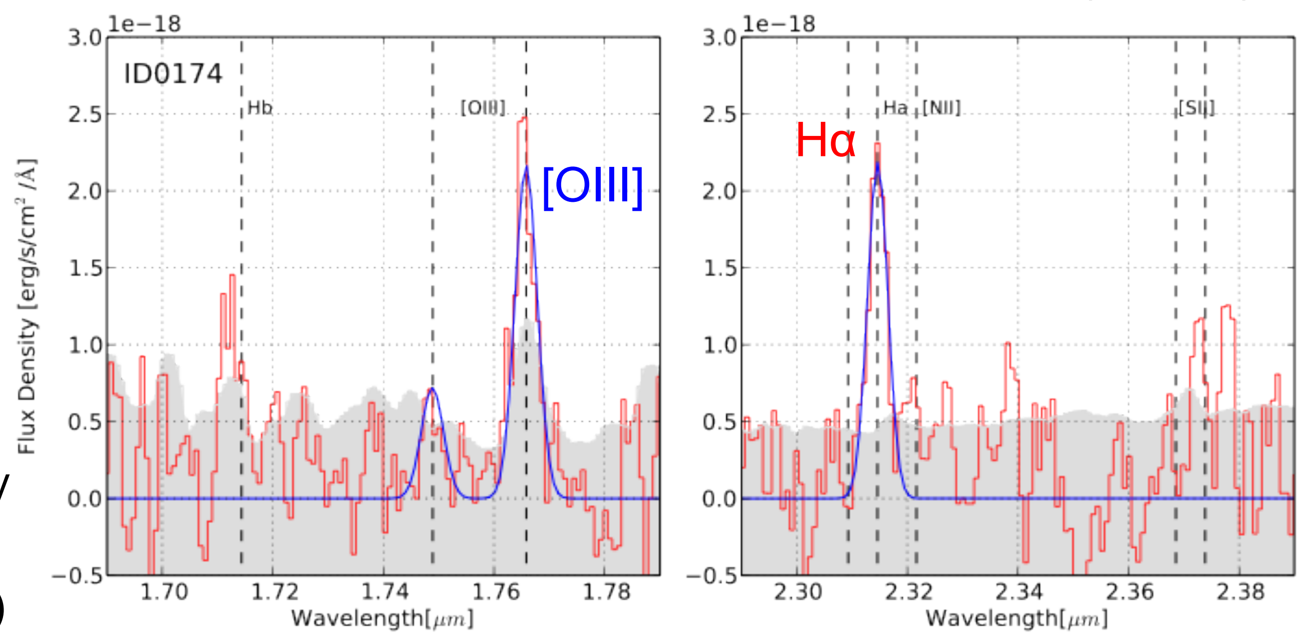

Deep MOIRCS spectroscopy of two proto-clusters at z>2

Shimakawa et al. (2013)

課題

形成最盛期にある銀河の、形態獲得、星形成、AGN、フィードバックが、「いつ」、「どこで」、「どのように」起き、どう「相互に関連」しているのか？

これらを「無バイアス」にかつ「統計的」に突き詰める。

1. バルジ形成の謎。クランプ移動か、銀河の合体か？
2. 銀河形成（星形成）のモード？継続的進化とバースト･フェーズの相対寄与は？
3. 星やガスの内部運動は？形態獲得との関係は？
4. 銀河のIMFは？時間変化？モード依存性？
5. 星形成活動とAGN活動とのリンクおよびフィードバック？
6. 遠方（特に低質量）銀河の物理状態？（[OIII]が強い理由）
7. これら全ての環境と質量への依存性は？なぜ？

SWIMS-18 Survey　基盤A (2012-2016)

２バンド同時観測＆広視野＆大量観測時間の特長を生かして、18枚もの多数のフィルターを搭載して、銀河形成最盛期の超多色＆広域撮像サーベイを行う！

Narrow-Band			Medium-Band				Broad-Band			
Band	λ_0(μm)	FWHM(μm)	Band	λ(μm)	λ_0(μm)	FWHM(μm)	Band	λ(μm)	λ_0(μm)	FWHM(μm)
NB1244	1.244	0.012	Y	1.00-1.10	1.05	0.10	J	1.17-1.33	1.25	0.16
※ NB1261	1.261	0.012	J1	1.11-1.23	1.17	0.12	H	1.48-1.78	1.63	0.30
NB1630	1.630	0.016	J2	1.23-1.35	1.29	0.12	Ks	1.99-2.30	2.15	0.30
NB1653	1.653	0.016	H1	1.44-1.56	1.50	0.12				
NB2137	2.137	0.021	H2	1.56-1.68	1.62	0.12				
NB2167	2.167	0.021	H3	1.68-1.80	1.74	0.12				
			K1	1.96-2.10	2.03	0.14				
			K2	2.10-2.24	2.17	0.14				
			K3	2.24-2.38	2.31	0.14				

※ HST F126N 1.259 0.015

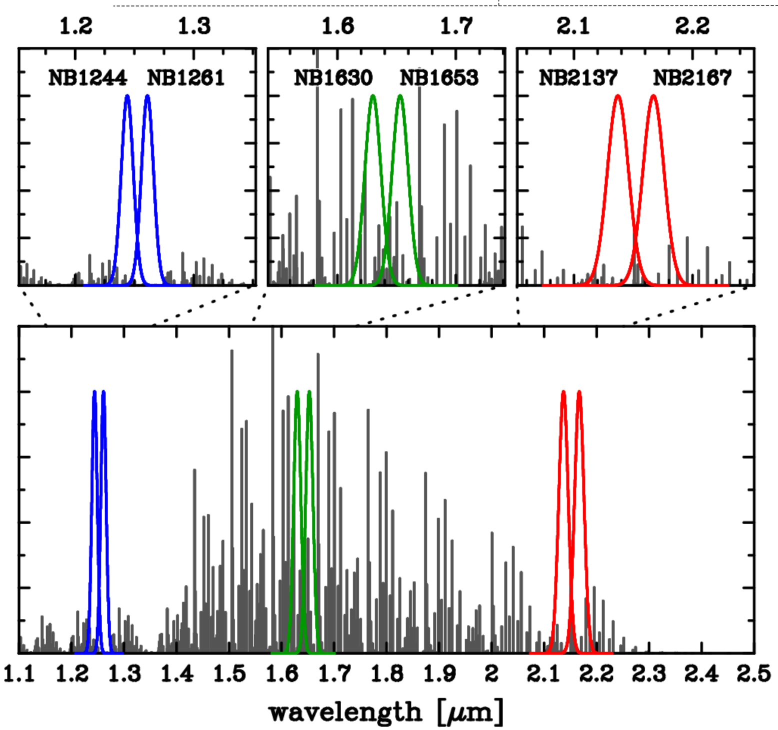

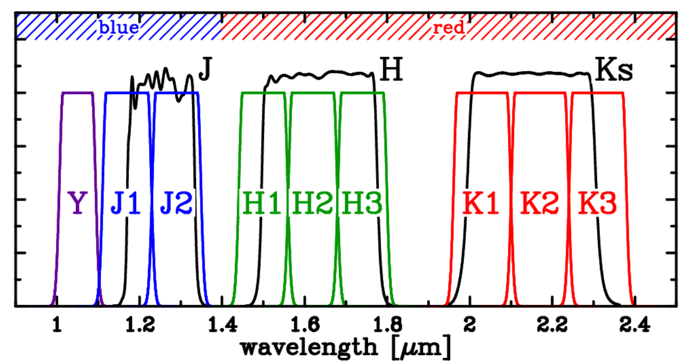

blue チャンネル	red チャンネル	
NB1244 (6h)	NB1630 (3h),	NB2137 (3h)
NB1261 (6h)	NB1653 (3h),	NB2167 (3h)
Y (3h)	H1 (2h),	K1 (1h)
J1 (3h)	H2 (2h),	K2 (1h)
J2 (3h)	H3 (2h),	K3 (1h)
J (1.5h)	H (1h),	Ks (0.5h)

Medium-band redshifts

● NEWFIRM medium-band data

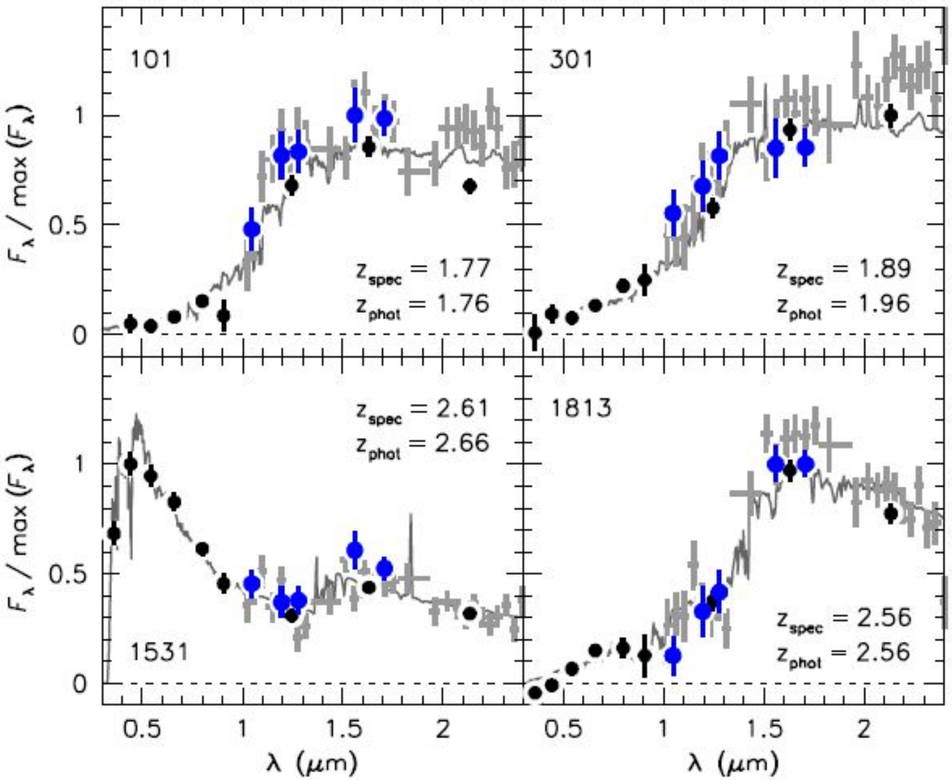

Fig. 2.— Spectral energy distributions from 0.3 – 2.4 μm of the four galaxies in the SDSS 1030 Kriek et al. (2008) sar the highest S/N ratio. Black points are broad band photometric data, blue points are the new medium band data. The med data are able to pinpoint the location of rest-frame optical breaks in the spectra. Dark grey spectra are the best-fit EAZ SEDs. Light grey points are binned near-IR spectra obtained with GNIRS on Gemini, from Kriek et al. The best-fit model the (independent!) GNIRS spectra very well.

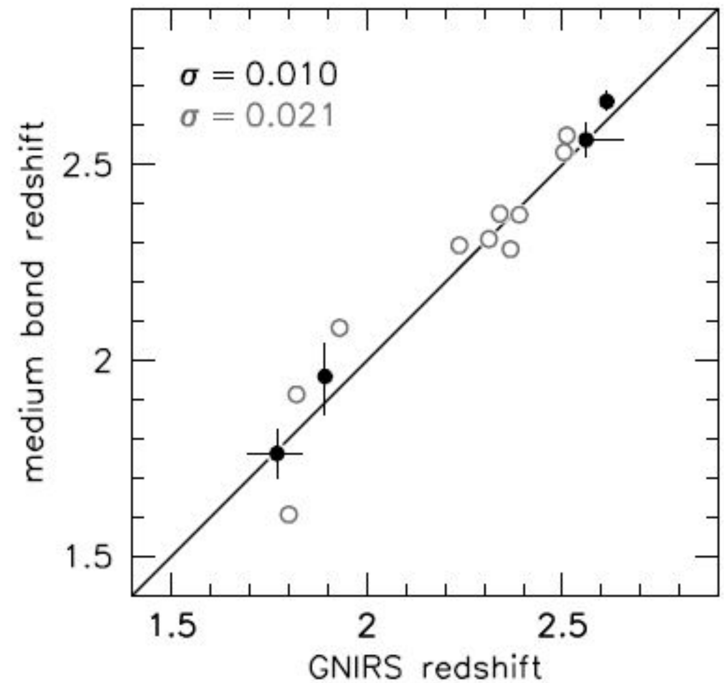

Fig. 3.— Comparison of photometric redshifts derived from medium band photometry to spectroscopic redshifts measured with the GNIRS near-IR spectrograph on Gemini for the four galaxies shown in Fig. 2 (solid symbols). There is very good agreement, with scatter 0.01 – 0.02 in $\Delta z/(1+z)$. Open symbols show the remaining 10 objects from the Kriek et al. (2008) sample. The scatter is small even for these galaxies, even though the S/N of their medium band photometry is lower than our survey criterion.

$\Delta z/(1+z) \sim 0.02$

van Dokkum et al. (2009), arXiv:0901.0551

SWIMS-18 NB emitters survey (z=0.9, 1.5, 2.5, 3.3)

Target redshifts for line emitters (NB)

	z(Hα)	z(OIII)	z(Hβ)	z(OII)	z(Paα)
NB1244	※0.895	1.484	1.559	2.337	
NB1261	※0.922	1.519	1.595	2.384	
NB1630	1.484	2.256	2.354		
NB1653	1.519	2.302	2.401		
NB2137	2.256	3.268			0.140
NB2167	2.302	3.328			0.156

A super-cluster
※ CL1604+4304(z=0.895)
※ CL1604+4321(z=0.920)

独創的なアイデア！

Dual Emitters (Hα and [OIII])

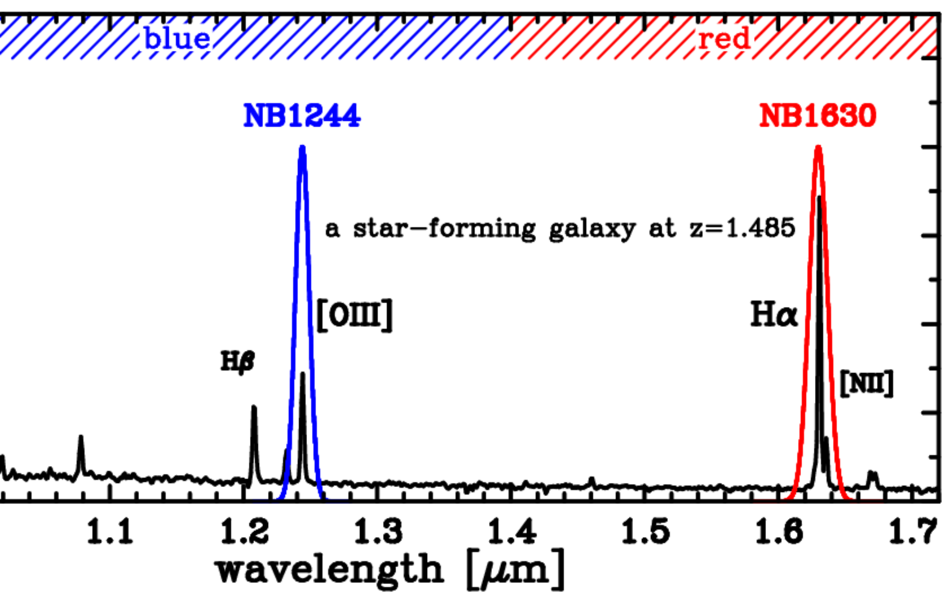

For Subaru (x1.6 for TAO)

blue チャンネル	red チャンネル	
NB1244 (6h)	NB1630 (3h),	NB2137 (3h)
NB1261 (6h)	NB1653 (3h),	NB2167 (3h)
Y (3h)	H1 (2h),	K1 (1h)
J1 (3h)	H2 (2h),	K2 (1h)
J2 (3h)	H3 (2h),	K3 (1h)
J (1.5h)	H (1h),	Ks (0.5h)

~25 hrs / FoV including overheads (40 hrs for TAO)

$M^* = 10^{10} M_\odot$ (z=1.5), $10^{11} M_\odot$ (z=4)

SFR (Hα) = 3, 10, 30 $M_\odot$/yr (z=0.9, 1.5, 2.5)

(1 mag extinction assumed)

Hα Emitter Survey on a Gigantic Super-Cluster at z~0.9

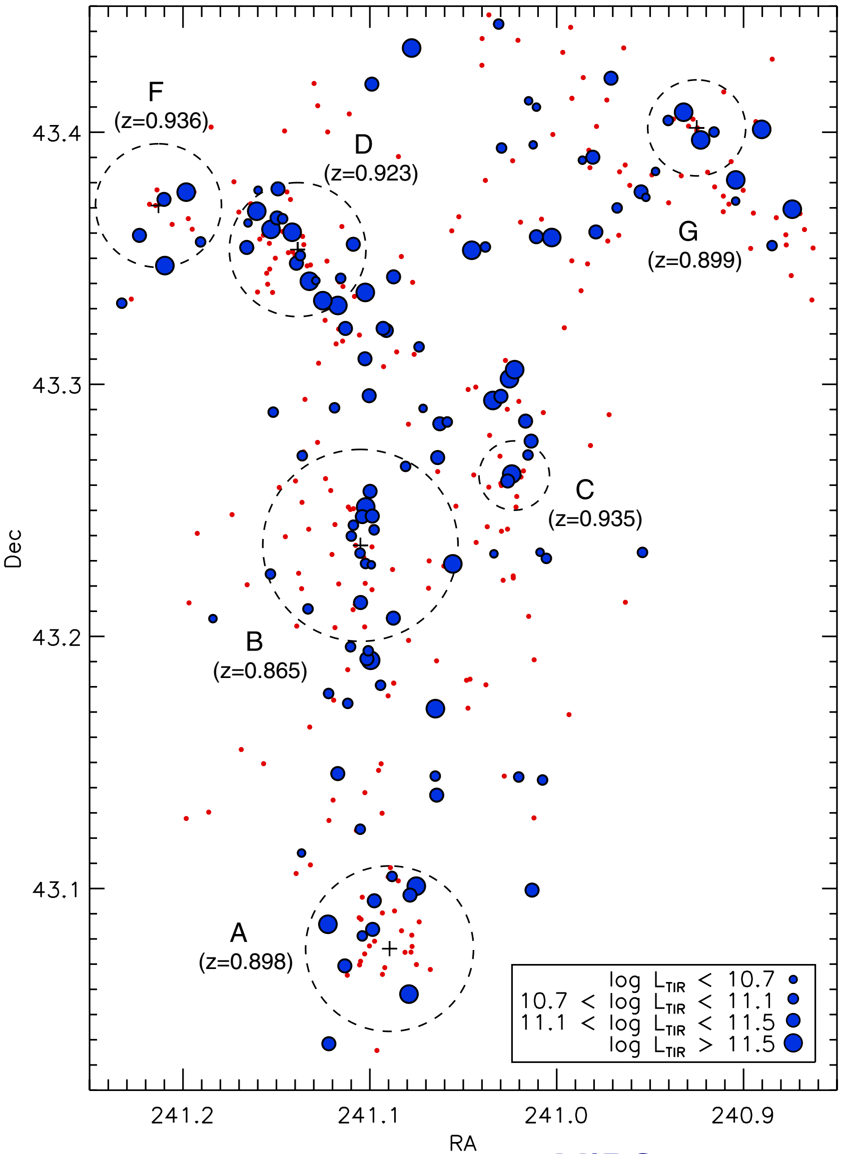

● MIPS sources

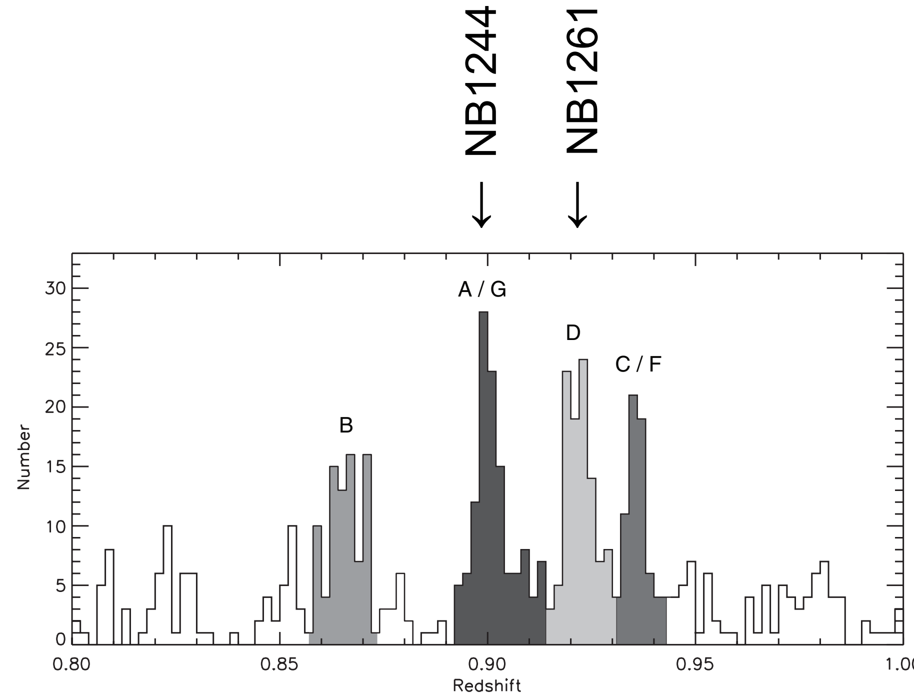

Figure 2. Redshift distribution of the Cl1604 supercluster.

Table 1
Properties of Galaxy Clusters and Groups in the Cl1604 Supercluster

ID	Name	R.A. (J2000)	Decl. (J2000)	z	σ_v (km s^{-1})	R_{vir} arcmin/(h_{70}^{-1} Mpc)	N_{gal} ($R < 2R_{vir}$)
A	Cl1604+4304	241.097473	43.081150	0.898	703 ± 110	1.969/0.92	40
B	Cl1604+4314	241.105050	43.239611	0.865	783 ± 74	2.261/1.05	62
C	Cl1604+4316	241.031623	43.263130	0.935	304 ± 36	0.824/0.39	13
D	Cl1604+4321	241.138651	43.353430	0.923	582 ± 167	1.594/0.75	60
F	Cl1605+4322	241.213137	43.370908	0.936	543 ± 220	1.470/0.70	16
G	Cl1604+4324	240.925080	43.401718	0.901	409 ± 86	1.143/0.53	15

Kocevski et al. (2011)

SWIMS-18

1平方度の広域、18フィルターの超多色撮像、z~4.5まで拡張

- Medium-band (9枚) のphot-z探査による、1<z<4.5における、準星質量リミットサンプル（特に受動的銀河）の構築とその進化の研究。$\Delta z/(1+z) < 0.02$
- Narrow-band (6枚) のHα／[OIII]輝線探査による、z=0.9, 1.5, 2.5, 3.4における、準星形成率リミットサンプルの構築とその進化の研究。低質量側に延長。AGNの寄与も明らかに。

→ 銀河の質量集積、星形成、BH成長の歴史を、

「無バイアス」かつ「統計的」に明らかにする！

Z-FOURGE @Magellan 6.5m (FourStar Galaxy Evolution Study)

- Four Star Infrared Camera; Hawaii-2RG x 4
- One deep 10.9'x10.9' field each in COSMOS, CDFS and UDS FourStar; Hawaii-2RG x 4)
- 30,000 galaxies at $1<z<3$
- J1,J2,J3 ≈ 25.5, Hl, Hs ≈ 25, and Ks ≈ 24.5 (AB, 5σ, total mag for compact sources)
- $\Delta z/(1+z) \sim 0.02$

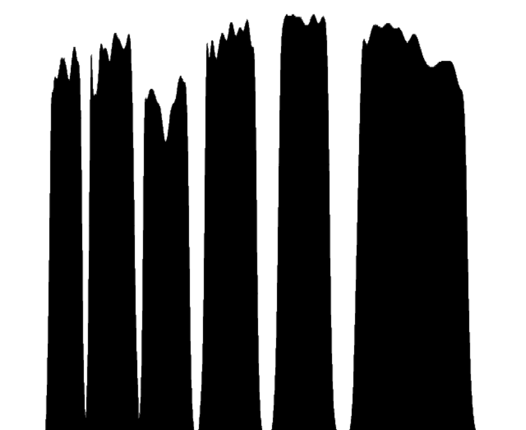

SWIMS-18がZ-FOURGEより優れている点

- Medium-band filtersの枚数増

  J1(Y),J2,J3,Hs,Hl,Ks　→　Y,J1,J2,H1,H2,H3,K1,K2,K3

  (Hを２から３分割へ。Kを１から３分割へ。計６から９枚へ。）

  → Phot-z精度(特にz>3)の向上、4<z<4.5銀河サンプルの構築（B-drop LBGと連携）

- Narrow-band filtersの存在

  6枚の狭帯域フィルター、Hαと[OIII]の２ラインを狙う3組のペア、オンバンドとオフバンドが隣接。

  → [OIII]の強い遠方銀河に最適化、よりクリーンなエミッター選択

- ２バンド同時観測

  λ<1.4μm (blue) と λ>1.4μm (red) とを同時観測。

  → サーベイ効率が2倍に！　但し、初期視野は3分の1。検出器倍増が必須。

- 観測時間の集中投資

  → 1.5年使って10倍広い視野（1平方度）を！ 原始銀河団(>$10^{14}M_{\odot}$)も入る。

Survey Design for SWIMS-18 (imaging)

- 1 sq. deg. (CANDELS, HSC-Ultra-Deep)　(SWIMS18-Wide)

  100 pointings (×25 hrs/FoV) = 4,000 hrs = 365 nights

  SFR-limit sample: 7.5×10^5 Mpc^3 at each redshift

  (Hα emitters)　3, 10, 30 $M_\odot$/yr (z=0.9, 1.5, 2.5)

  ~16,000, 8,000, 4,000 HAEs (同上)

  M*-limit sample: 1.2×10^7 Mpc^3 (Δz=1)

  $M^* = 10^{10} M_\odot$ (z=1.5), $10^{11} M_\odot$ (z=4) ~ 100個

- このうち 0.1 sq. deg.では、5倍の積分時間　(SWIMS18-Deep)

→ TAOのおよそ1.5 年間分の観測時間を投入すればよい。

（SWIMSの視野を2倍にできれば、半分の時間または倍の視野）

Subaru搭載時（2015−2017）にはこの1/10規模をパイロットサーベイとして実行

Spectroscopic follow-up of SWIMS-18

PFS (optical) + SWIMS (NIR)

- Accurate physical quantities
  - Spec-z and 3D structures
  - Dust corrected SFRs (Hα/Hβ)
  - Gaseous metallicity (R23, O32, N2)
  - AGN separation ([OIII]/Hβ vs. [NII]/Hα)
  - Composite spectra of red galaxies (post-starburst)
- SWIMS-IFU
  - Kinematics (rotation/random/outflows)
  - Central AGN
  - Star forming regions